J. Fluid Mech. (1964), *vol.* 20, *part* 1, *pp.* 141–159
Printed in Great Britain

A theory for the mode of operation of the Hartmann air jet generator

By K. A. MØRCH
Fluid Mechanics Department, Technical University of Denmark, Copenhagen

(Received 4 July 1963 and in revised form 6 April 1964)

The Hartmann air jet generator (Hartmann 1939) is a sound wave generator in which the sound is generated by oscillations of a shock developed in an over-expanded air jet by means of a blunt body: a resonator. A theory for the instability mechanism is advanced, and it is found that the results calculated from the theory are in good agreement with the experimental observations.

1. Introduction

The Hartmann generator is made of an axially symmetrical convergent nozzle and a resonator (figure 1). Axially symmetrical resonators of different size and form can be used. The resonator with bore shown in figure 1 was used by Hartmann (1939) to obtain a high acoustical efficiency of the generator. During the investigations presented here plane resonators, i.e. resonators without bore, but with plane terminal surface, were principally used.

The frequency and the acoustic power of the generator depends on the diameter of the nozzle d_n, the resonator type, the resonator/nozzle ratio d_r/d_n, the distance from nozzle to resonator x_{res} and on the stagnation pressure p_0 of the air supplied to the generator.

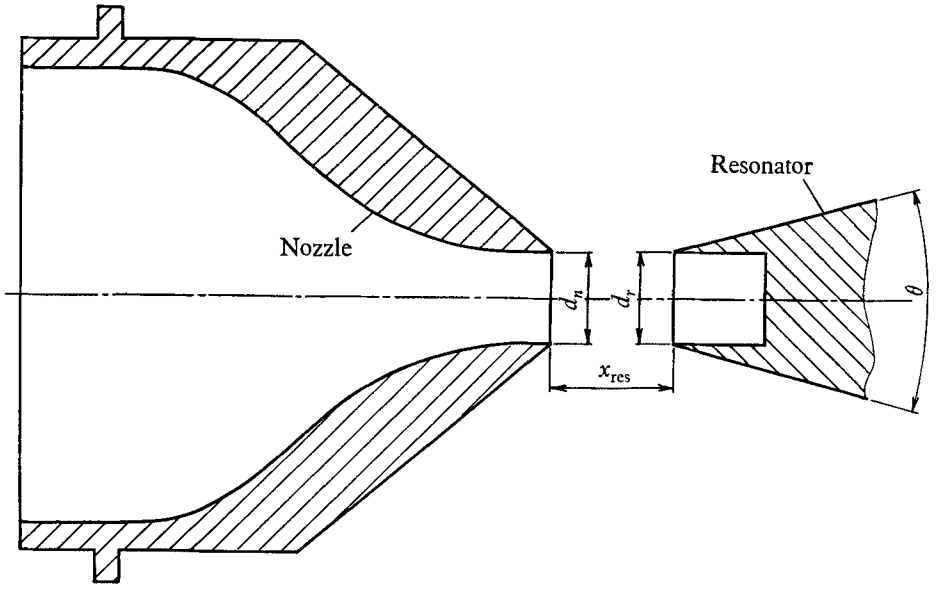

FIGURE 1. Hartmann generator (resonator with bore).

In the free supersonic air jet, i.e. the air jet without resonator, a shock will be created at some distance from the nozzle by convergence of Mach lines. This Mach shock is stable, but if a resonator is inserted into the jet at such a position that a blunt body shock—the resonator shock— is produced in the supersonic jet upstream of the position where the Mach shock is created in the free jet, then shock instability may occur.

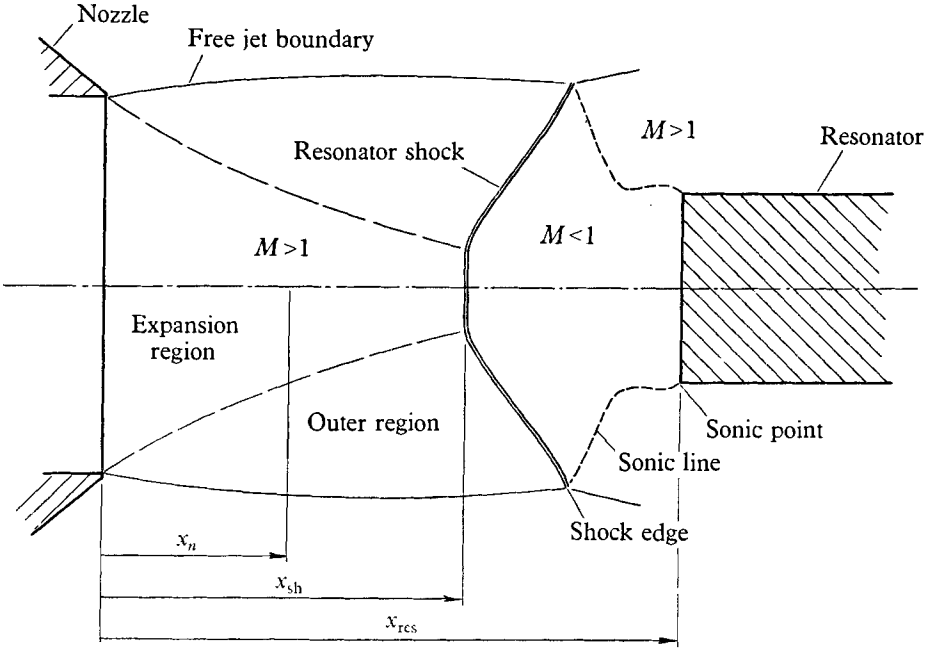

FIGURE 2. Flow pattern in the Hartmann generator.

2. Experimental investigations

The experimental investigations of the Hartmann generator were carried out with a 12·0 mm nozzle. A stagnation pressure p_0 determined by $p_B/p_0 = 0{\cdot}261$ (p_B = atmospheric pressure) was chosen for all experiments.

When the distance between nozzle and resonator x_{res}, and thus the distance between nozzle and shock x_{sh}, exceeds a certain value the shock produces periodic oscillations of large amplitude. For the case of a 12·3 mm resonator with 12·0 mm bore the course of one oscillation is shown in figure 3, plate 1. The pictures show that between the oscillating resonator shock and the bottom of the resonator a secondary shock wave travels. Measurement of the pressure oscillation at the bottom of the resonator with a quartz transducer also indicates that reflexion of a shock wave occurs.

Instability of the same type is found with plane resonators. The only difference is an increase of frequency and a decrease of shock amplitude.

If x_{res} is smaller than the above-mentioned limit the large amplitude shock oscillations do not occur, and it is then found that the shock form and position are almost independent of whether a resonator with or without bore is used. Further, the angle θ (figure 1) is unimportant if the position of sonic point at the

resonator surface is at the sharp front edge of the resonator. This implies that θ must not be too large. The parameter which is decisive for the shock form and position is the resonator diameter at sonic point. This is equivalent to what is found for blunt body shocks in parallel flows (Vaglio-Laurin 1962).

The shock-resonator positions are given in figure 4 for plane resonators of different diameters. The shock positions x_{sh} are measured in the axis from nozzle

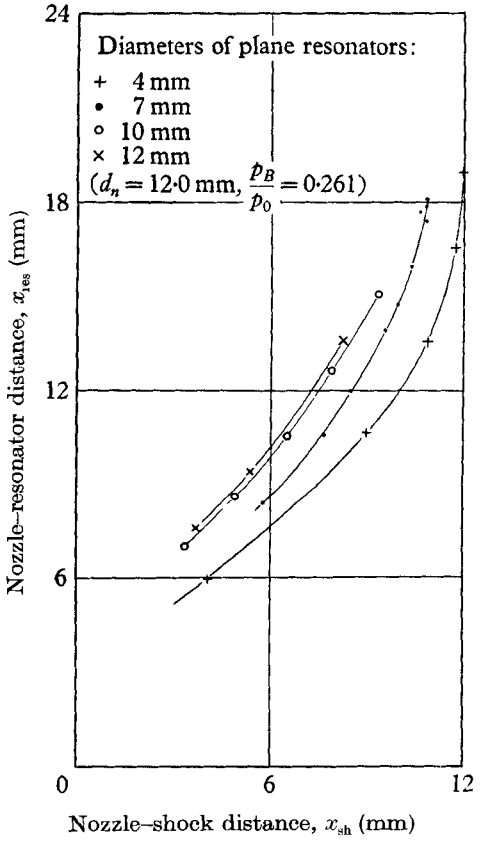

FIGURE 4. Shock-resonator positions for plane resonators of different diameters inside region of stability and weak instability (mean shock positions in case of unstable shocks).

to shock. The curves are shown to the point where large amplitude shock oscillations start. During the investigations with plane resonators, however, it was noticed that weak instabilities can occur inside the apparently stable region. The amplitude of oscillation for the resonator shock at these instabilities is very small. In the subsonic region behind the resonator shock small pressure oscillations are produced and these oscillations are able to create a weak oscillating oblique shock in the outer part of the jet downstream of the resonator shock (figure 5, plate 1) where the velocity has again become supersonic (figure 2).

With a 7·0 mm plane resonator, pressure oscillations at the resonator plane were registered with a built-in quartz transducer. Oscillograms of the pressure oscillations are shown in figure 6. It is found that the pressure oscillations may be

composed by two superimposed frequencies, but normally one frequency is dominating. The dominating frequencies are shown in figure 7 (*a*). The curve of lowest frequency corresponds to large amplitude shock oscillations ($x_{\text{res}} > 18{\cdot}1$ mm) and the other frequency curves to small amplitude shock oscillations. The corresponding pressure oscillations at the resonator plane are shown in figure 7 (*b*).

It is reasonable to assume that the mechanism of instability is a resonance phenomenon. In the central region of the jet, the resonator shock is practically

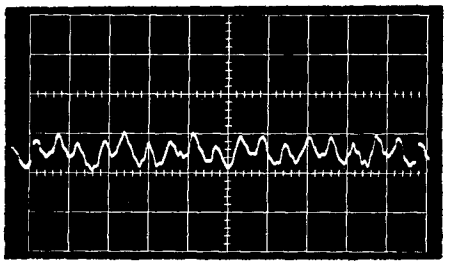

(*a*)

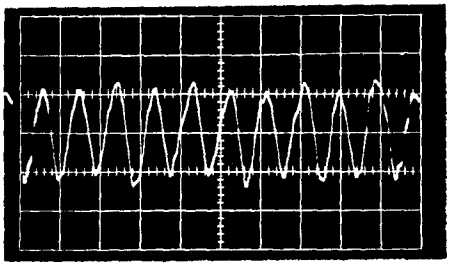

(*b*)

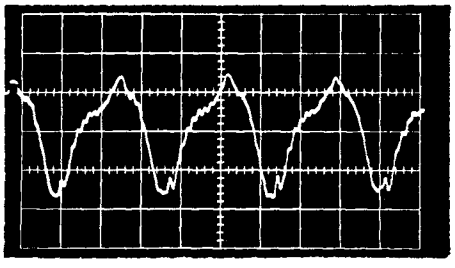

(*c*)

FIGURE 6. Oscillograms of pressure oscillations at the resonator plane for 7·0 mm plane resonator (x-sweep: 50 μsec/div). (*a*) $x_{\text{res}} = 14{\cdot}8$ mm, $\nu_m = 35$ kc/s; (*b*), (*c*) $x_{\text{res}} = 18{\cdot}1$ mm (jump position), $\nu_m = 21{\cdot}5$, 7·24 kc/s.

a normal shock—at least if it is not too near to the nozzle (figure 8, plate 2)—and during its oscillations nearly plane waves must be emitted into the subsonic region between resonator and shock. These waves will be reflected from the plane terminal surface of a plane resonator or from the bottom of the bore in case of a resonator with bore. When the waves return to the shock adaptation is necessary for the shock oscillation to continue. The time τ used for a wave to travel from the shock to the reflecting surface and back to the shock depends on the distance between shock and reflecting surface and accordingly the resonance frequencies must be different for a plane resonator and a resonator with bore and for plane resonators of different diameters.

The over-expanded supersonic air jet in the Hartmann generator is character-

FIGURE 3. The course of one oscillation in the Hartmann generator with 12·3 mm resonator with bore 12·0 × 12·0 mm. $\nu_m = 4{\cdot}5$ kc/s, $x_{\text{res}} = 16{\cdot}0$ mm.

FIGURE 5. The course of one oscillation in the Hartmann generator with 6·5 mm plane resonator (weak instability). Amplitude of oscillation for the resonator shock *c.* 0·2 mm. $\nu_m = 22$ kc/s, $x_{\text{res}} = 17{\cdot}6$ mm.

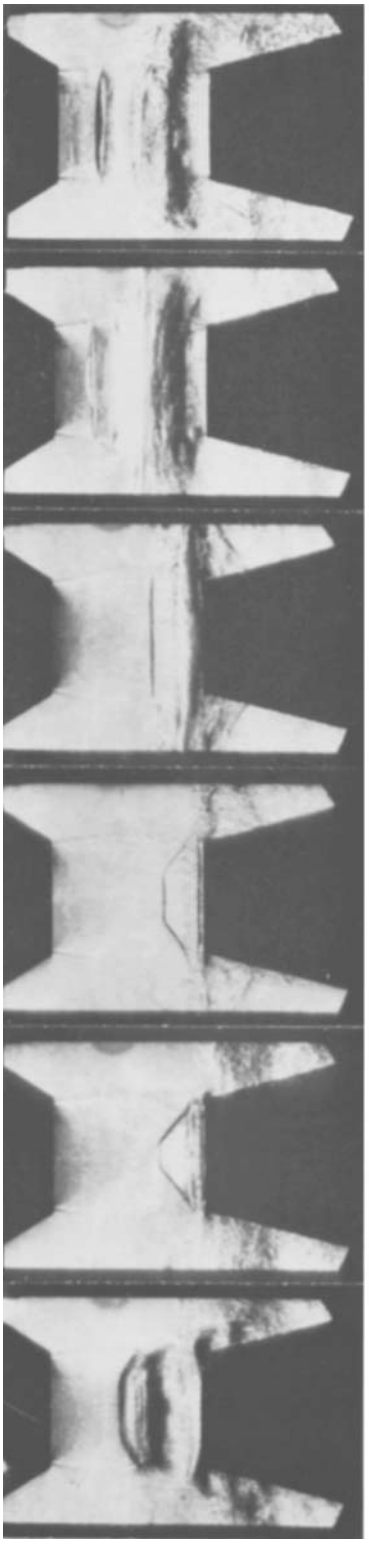

FIGURE 3

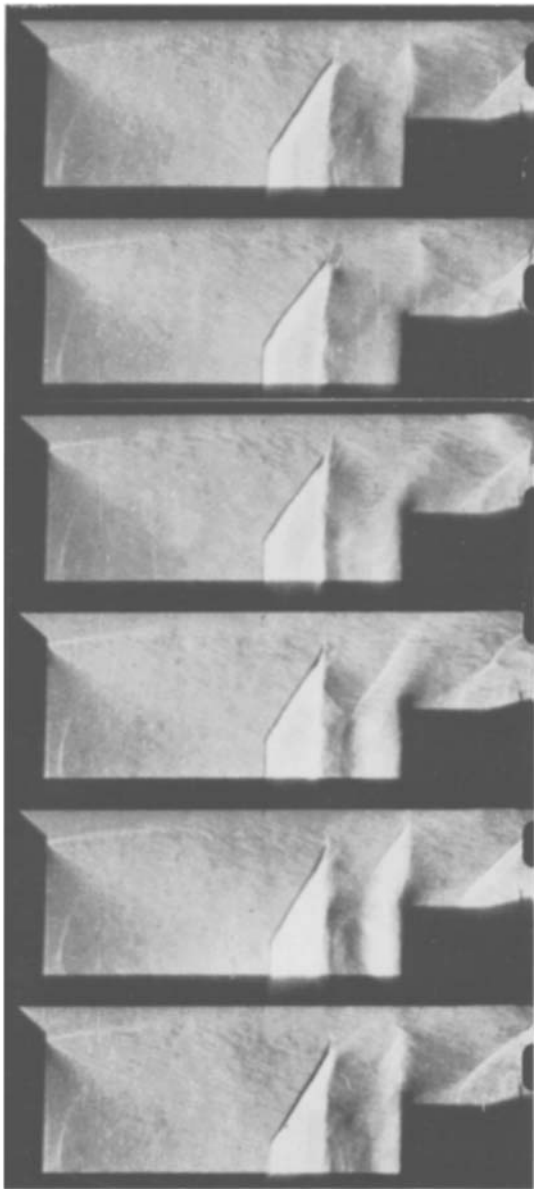

FIGURE 5

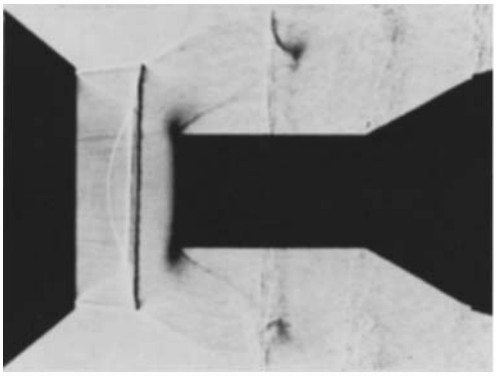

(*a*)

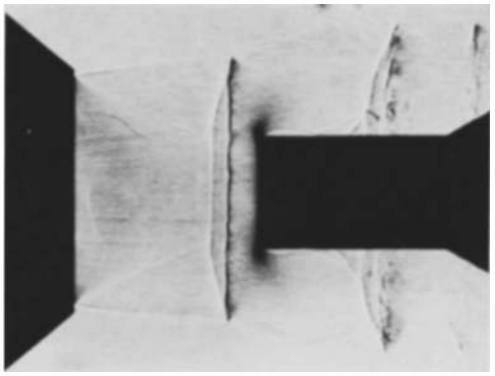

(*b*)

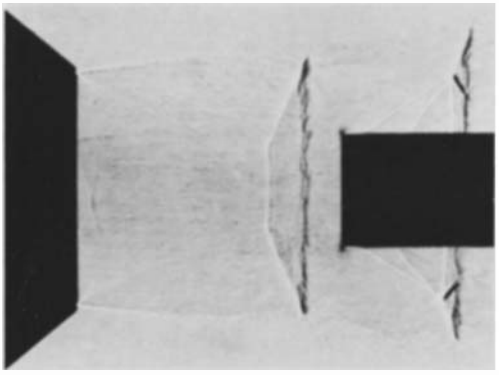

(*c*)

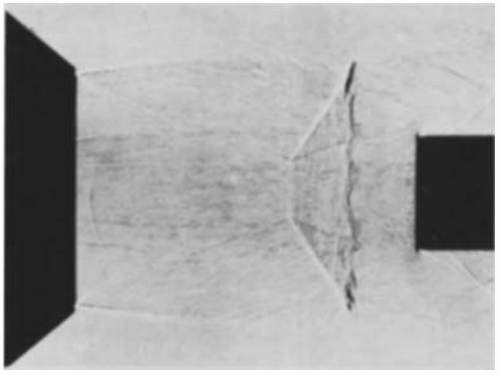

(*d*)

FIGURE 8. Schlieren photos of generator with 6·0 mm plane resonator. (*a*) x_{res} = 5·1 mm; (*b*) x_{res} = 9·5 mm; (*c*) x_{res} = 13·5 mm; (*d*) x_{res} = 17·5 mm.

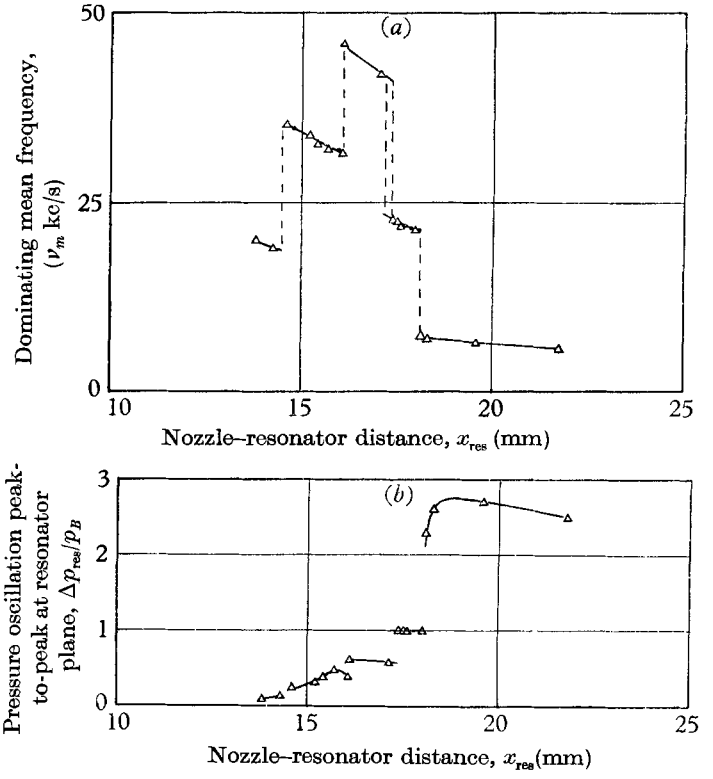

FIGURE 7. (*a*) Dominating mean frequencies ν_m for 7·0 mm plane resonator measured at the resonator plane. (*b*) Pressure oscillations at the resonator plane.

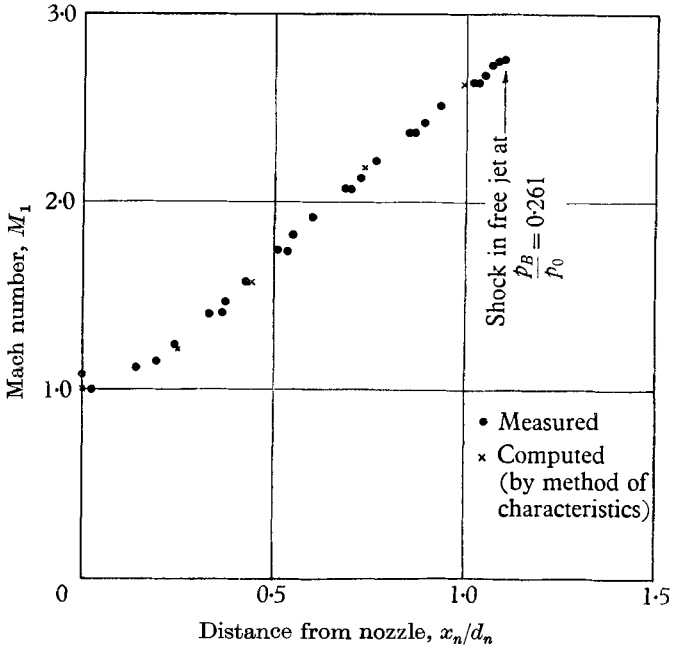

FIGURE 9. Mach number in the axis of the free jet.

ized by a varying Mach number in the direction of the axis as well as in cross-sections perpendicular to the axis. The Mach number in the axis of the free jet used for the investigations is shown in figure 9, and in figure 10 it is given for some cross-sections of the jet. It is seen that in the region near to the axis the Mach number varies essentially only in the axial direction and here the flow is *nearly* parallel.

For distances from nozzle to shock below about 7–8 mm ($x_{sh}/d_n \simeq 0{\cdot}6$), i.e., for Mach numbers in front of the shock below about 2·0, resonance phenomena

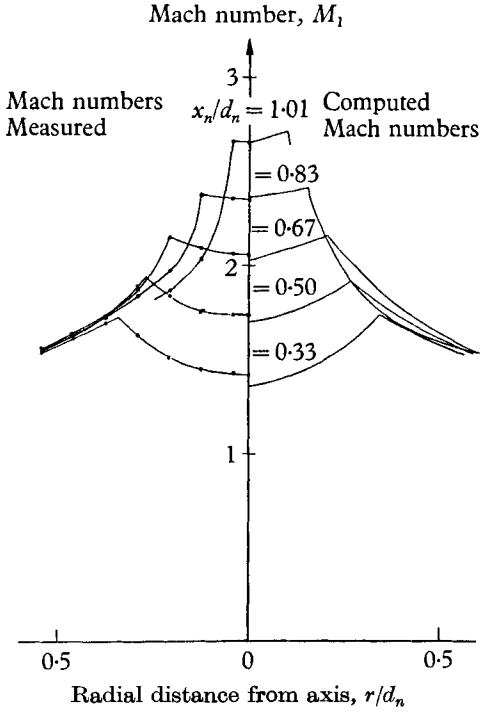

FIGURE 10. Measured and computed Mach numbers in cross-sections of the free jet.

have been registered only in a few cases and in these cases strong resonance never occurs.

The maximum Mach number in the axis of the free jet for the case treated was about 2·7—when this Mach number is reached the Mach shock occurs. The Mach shock is displaced in the downstream direction if the stagnation pressure p_0 is increased.

Thus resonance phenomena can be expected to occur for Mach numbers in front of the resonator shock given by $2{\cdot}0 < M_1 < M_{1,\max} \simeq 2{\cdot}7$.

3. Theory of instability

3.1. *The instability model*

A complete theoretical treatment of the instability problem is extremely difficult and a simplified model is used. As mentioned above, the flow in the region near to the generator axis can be expected to be of fundamental importance for the

occurrence of resonance and therefore only this part of the jet is considered. To further simplify the problem the case of a generator having a plane resonator is treated.

In the instability model the Mach number of the supersonic jet is thought to change only in the flow direction (figure 9). The jet is directed at the plane resonator. The resonator shock is a normal shock, the equilibrium position (detach-

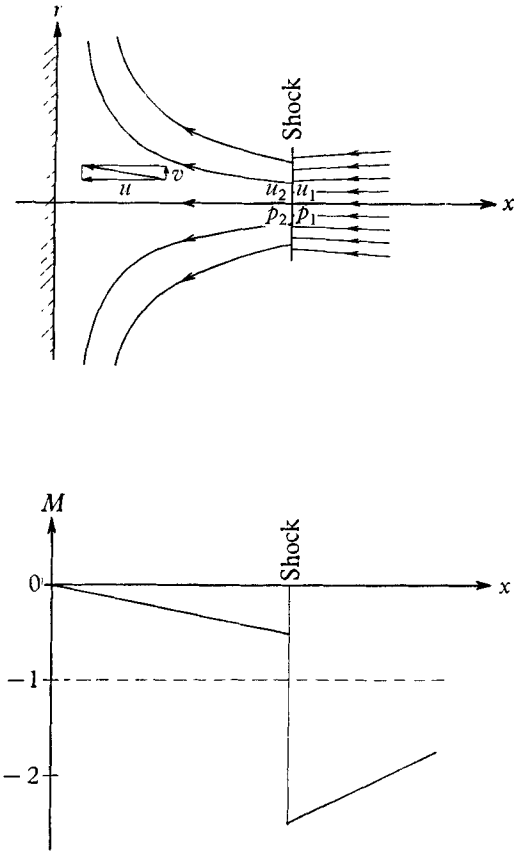

FIGURE 11. Stagnation flow.

ment distance) of which is determined by the resonator diameter. In the central region between the shock and the resonator the flow is a stagnation flow (figure 11).

If the normal shock carries out small oscillations in the axial direction, the pressure and velocity perturbations behind the shock will move as plane waves downstream to the resonator and after reflexion return to the shock. To find the conditions of resonance it is necessary (i) from the normal shock relations to compute the pressure and velocity perturbations behind the oscillating shock, (ii) to deduce the wave equation for perturbations in a stagnation flow and to find the solutions to this equation.

3.2. *Perturbations behind an oscillating normal shock*

If the normal shock oscillates sinusoidally at a frequency ω the displacement of the shock from the mean position is given by

$$\Delta x = l \sin \omega t. \tag{1}$$

In the mean position the Mach number just in front of the shock is M_1 and the static pressure is p_1. If the shock oscillates with a small amplitude l the Mach number in front of it is

$$M(x) = M_1 + \frac{dM_1}{dx} l \sin \omega t, \tag{2}$$

and the strength of the shock is given by

$$M_{1,\mathrm{sh}} = M_1 + \frac{dM_1}{dx} l \sin \omega t - \frac{\omega l}{a_1} \cos \omega t = M_1 + \Sigma \Delta M. \tag{3}$$

(The index sh denotes that the system of co-ordinates is attached to the shock.)

Pressure perturbation

The static pressure just in front of the oscillating normal shock is given by

$$p(x) = p_1 + \frac{dp_1}{dx} l \sin \omega t. \tag{4}$$

With the equations for adiabatic flow, the normal shock equations (Liepmann & Roshko 1957), and the assumption of small amplitudes, l, it is found that the static pressure just behind the shock is

$$p_2 = p_1 \left(1 + \frac{2\gamma}{\gamma+1} \{(M_1 + \Sigma \Delta M)^2 - 1\}\right) \left(1 + \frac{\gamma M_1}{1 + \frac{1}{2}(\gamma-1) M_1^2} \frac{dM_1}{dx} l \sin \omega t\right). \tag{5}$$

The static pressure behind the shock can be regarded as composed of a stationary part p_{2s} and a non-stationary part p_{2n}

$$p_2 = p_{2s} + p_{2n}.$$

Excluding small second-order terms and using $(\gamma-1)/2\gamma \ll M_1^2$ it is found that

$$p_{2n} = p_1 \frac{2\gamma}{\gamma+1} M_1 \left(\frac{2 - M_1^2}{1 + \frac{1}{2}(\gamma-1) M_1^2} \frac{dM_1}{dx} l \sin \omega t - \frac{2\omega l}{a_1} \cos \omega t\right), \tag{6}$$

where a_1 is the velocity of sound in front of the shock.

Velocity perturbation

The velocity perturbation behind the oscillating normal shock can be found from equation (3) and the normal shock equation

$$u_{2,\mathrm{sh}} = \left(\frac{\gamma-1}{\gamma+1} + \frac{2}{\gamma+1} \frac{M_1 - 2\Sigma \Delta M}{M_1^3}\right) a_1 (M_1 + \Sigma \Delta M). \tag{7}$$

In the system of co-ordinates fixed to the resonator the velocity perturbation is

$$u_2 = u_{2,\mathrm{sh}} + \omega l \cos \omega t,$$

and expressing u_2 as the sum of a stationary part u_{2s} and a non-stationary part u_{2n}

$$u_2 = u_{2s} + u_{2n},$$

it is found that

$$u_{2n} = \left(\frac{\gamma-1}{\gamma+1} - \frac{2}{\gamma+1}\frac{1}{M_1^2}\right) a_1 \Sigma \Delta M + \omega l \cos \omega t. \tag{8}$$

In the Hartmann generator resonance is registered for $2{\cdot}0 < |M_1| < 2{\cdot}7$ and therefore the first term in equation (8) is insignificant compared with the last term. Accordingly

$$u_{2n} = \omega l \cos \omega t. \tag{9}$$

3.3. *The wave equation for plane perturbations in a stagnation flow*

It is convenient for the theoretical computations to use a system of co-ordinates with starting-point in the centre of the resonator plane and with the x-axis directed upstream (figure 11). This implies that the axial flow velocities become negative. The equations for axially symmetrical flow (Schlichting 1960) are used, and the circumferential velocity is put equal to zero.

As the thickness of the boundary layer at the resonator plane is very small compared with the distance from resonator to shock it can be neglected. In the region near the axis the frictional forces occur only in the boundary layer at the resonator, so that the frictional terms in the Navier-Stokes equations can therefore be omitted, giving

$$\rho\left(\frac{\partial u}{\partial t} + u\frac{\partial u}{\partial x} + v\frac{\partial u}{\partial r}\right) = -\frac{\partial p}{\partial x}, \tag{10}$$

and

$$\rho\left(\frac{\partial v}{\partial t} + u\frac{\partial v}{\partial x} + v\frac{\partial v}{\partial r}\right) = -\frac{\partial p}{\partial r}, \tag{11}$$

while the equation of continuity is

$$\frac{\partial \rho}{\partial t} + \frac{\partial}{\partial x}(\rho u) + \frac{\partial}{\partial r}(\rho v) + \frac{\rho v}{r} = 0. \tag{12}$$

As the Mach number in front of the shock $|M_1| > 2{\cdot}0$ in the regions where resonance normally occurs, the Mach number just behind the shock $|M_2| < 0{\cdot}58$, and therefore the compressibility effects are small in the stationary stagnation flow between shock and resonator, and the flow velocities found for incompressible flow can be used for the stationary basic flow (Schlichting 1960; Vaglio-Laurin 1962):

$$u_s = \alpha x, \quad v_s = -\tfrac{1}{2}\alpha r. \tag{13), (14}$$

For this flow equations (10) and (11) give

$$\alpha^2 x \rho_s = -\partial p_s/\partial x, \quad \tfrac{1}{4}\alpha^2 r \rho_s = -\partial p_s/\partial r. \tag{15), (16}$$

Now a plane perturbation (index p) moving along the x-axis and given by the velocity potential

$$u_p = -\partial \phi/\partial x \tag{17a}$$

is superposed on the stagnation flow (Stewart & Lindsay 1930):

$$u = u_s + u_p = \alpha x - \partial \phi/\partial x. \tag{17b}$$

From equation (10) it is found that

$$\rho\left\{-\frac{\partial^2\phi}{\partial x\,\partial t}+\left(\alpha x-\frac{\partial\phi}{\partial x}\right)\frac{\partial}{\partial x}\left(\alpha x-\frac{\partial\phi}{\partial x}\right)\right\}=-\frac{\partial p}{\partial x}. \tag{18}$$

In this equation ρ can be regarded as constant and by first integrating with respect to x and then differentiating with respect to t and assuming that

$$|\alpha x| \gg |\partial\phi/\partial x|, \tag{19}$$

it is found that

$$\rho\left(\frac{\partial^2\phi}{\partial t^2}+\alpha x\frac{\partial^2\phi}{\partial x\,\partial t}\right)=\frac{\partial p}{\partial t}. \tag{20}$$

The static pressure p and the density ρ have stationary and non-stationary components:

$$p=p_s+p_p, \quad \rho=\rho_s+\rho_p. \tag{21), (22}$$

Equation (12) can be divided in a stationary component associated with the basic flow and a non-stationary component:

$$\left[\frac{\partial}{\partial x}(\rho_s u_s)+\frac{\partial}{\partial r}(\rho_s v_s)+\frac{\rho_s v_s}{r}\right]$$
$$+\left[\frac{\partial\rho_p}{\partial t}+\frac{\partial}{\partial x}(\rho_s u_p+\rho_p(u_s+u_p))+\frac{\partial}{\partial r}(\rho_p v_s)+\frac{\rho_p v_s}{r}\right]=0. \tag{23}$$

The basic flow component contained in the first square bracket is identically zero and the remainder of the equation can be rewritten

$$\frac{\partial\rho_p}{\partial t}+(u_s+u_p)\frac{\partial\rho_p}{\partial x}+u_p\frac{\partial\rho_s}{\partial x}+v_s\frac{\partial\rho_p}{\partial r}$$
$$+\frac{\rho_p}{\rho_s}\left[\rho_s\frac{\partial u_s}{\partial x}+\rho_s\frac{\partial v_s}{\partial r}+\frac{\rho_s v_s}{r}\right]+(\rho_s+\rho_p)\frac{\partial u_p}{\partial x}=0. \tag{24}$$

The compressibility of the stationary basic flow cannot be neglected when it appears in association with the perturbation, because although it is small it is of the same order of magnitude as the density perturbation ρ_p. Accordingly the square bracket in equation (24) must be transformed with equation (12) before equations (13) and (14) can be inserted:

$$\frac{\partial\rho_p}{\partial t}+(u_s+u_p)\frac{\partial\rho_p}{\partial x}+u_p\frac{\partial\rho_s}{\partial x}+v_s\frac{\partial\rho_p}{\partial r}$$
$$+\frac{\rho_p}{\rho_s}\left[-u_s\frac{\partial\rho_s}{\partial x}-v_s\frac{\partial\rho_s}{\partial r}\right]+(\rho_s+\rho_p)\frac{\partial u_p}{\partial x}=0. \tag{25}$$

In the region near to the axis v_s is small and thus also $\partial\rho_s/\partial r$ is small. Further the perturbation introduced by equation (17a) has no r-component, which gives $\partial\rho_p/\partial r=0$. Equation (25) can now be reduced to

$$\frac{\partial\rho_p}{\partial t}+\alpha x\frac{\partial\rho_p}{\partial x}-\left(\frac{\partial\phi}{\partial x}+\frac{\rho_p}{\rho_s}\alpha x\right)\frac{\partial\rho_s}{\partial x}-\rho\frac{\partial^2\phi}{\partial x^2}=0. \tag{26}$$

With $c^2 = \partial p_p/\partial \rho_p$ equations (15) and (18) give

$$\frac{\partial \rho_p}{\partial x} = \frac{\rho}{c^2}\left(\frac{\partial^2 \phi}{\partial x\,\partial t} + \alpha x \frac{\partial^2 \phi}{\partial x^2} + \alpha \frac{\partial \phi}{\partial x}\right) - \frac{\rho_p}{c^2}\alpha^2 x. \tag{27}$$

Equation (20), with equations (15), (26), (27) and $\rho_s \simeq \rho$, gives

$$\frac{\partial^2 \phi}{\partial t^2} + 2\alpha x \frac{\partial^2 \phi}{\partial x\,\partial t} - (c^2 - \alpha^2 x^2)\frac{\partial^2 \phi}{\partial x^2} + 2\alpha^2 x \frac{\partial \phi}{\partial x} = 0, \tag{28}$$

which is the wave equation for a stagnation flow.

The coefficients in equation (28) depend only on x and the solutions must have the form

$$\phi = e^{\sigma t} F(x), \tag{29}$$

and the complete solution can be written

$$\phi = e^{\sigma t}(C_A F_A + C_B F_B), \tag{30}$$

where C_A and C_B are constants. Introducing equation (29) into equation (28) the latter is reduced to an ordinary differential equation of hypergeometric type (Kamke 1942),

$$(c^2 - \alpha^2 x^2)\frac{d^2 F}{dx^2} - 2(\sigma + \alpha)\alpha x \frac{dF}{dx} - \sigma^2 F = 0. \tag{31}$$

With
$$\mu = -\sigma/\alpha = -(\sigma_r + i\sigma_i)/\alpha = \eta + i\xi, \tag{32}$$

and
$$2\chi = (\alpha x/c) + 1, \tag{33}$$

equation (31) is transformed into

$$\chi(\chi - 1)\frac{d^2 F}{d\chi^2} + [(2 - 2\mu)\chi - (1 - \mu)]\frac{dF}{d\chi} + \mu^2 F = 0. \tag{34}$$

A solution to this equation is given by

$$F_A(p, q, r, \chi) = 1 + \sum_{n=1}^{\infty} \frac{p(p+1)\dots(p+n-1)}{n!}\frac{q(q+1)\dots(q+n-1)}{r(r+1)\dots(r+n-1)}\chi^n, \tag{35}$$

where
$$p + q + 1 = 2 - 2\mu, \quad r = 1 - \mu, \quad pq = \mu^2,$$

from which
$$\left.\begin{matrix} p \\ q \end{matrix}\right\} = \tfrac{1}{2} - \mu \pm (\tfrac{1}{4} - \mu)^{\frac{1}{2}}.$$

Then equation (35) can be written

$$\begin{aligned} F_A(\chi) &= 1 + \sum_{n=1}^{\infty} \frac{\mu^2(2 + \mu^2 - 2\mu)\dots((\mu - n)^2 + 2\mu - n)}{n!\,(1-\mu)\,(2-\mu)\dots(n-\mu)}\chi^n \\ &= 1 + \sum_{n=1}^{\infty} A_{n-1}\frac{(\mu - n)^2 + 2\mu - n}{n(n-\mu)}\chi, \end{aligned} \tag{36}$$

where A_{n-1} denotes the $(n-1)$th term of the series and $A_0 = 1$.

A second solution is

$$\begin{aligned} F_B(\chi) &= \chi^{1-r} F(p - r + 1, q - r + 1, 2 - r, \chi) \\ &= \chi^{\mu} + \sum_{n=1}^{\infty} \frac{(p+\mu)\,(p+\mu+1)\dots(p+\mu+n-1)}{n!} \\ &\qquad \times \frac{(q+\mu)\,(q+\mu+1)\dots(q+\mu+n-1)}{(1+\mu)\,(2+\mu)\dots(n+\mu)}\chi^{n+\mu}, \end{aligned}$$

which can be rewritten

$$F_B(\chi) = \chi^\mu \left(1 + \sum_{n=1}^{\infty} \frac{\mu(2+\mu)\dots(n^2-n+\mu)}{n!\,(1+\mu)\,(2+\mu)\dots(n+\mu)}\chi^n\right)$$

$$= \chi^\mu \left(1 + \sum_{n=1}^{\infty} B_{n-1}\frac{n^2-n+\mu}{n(n+\mu)}\chi\right), \tag{37}$$

where B_{n-1} denotes the $(n-1)$th term and $B_0 = 1$.

3.4. *Equations for determination of resonance*

A plane perturbation was defined by the velocity potential equation (17*a*). The corresponding pressure potential is found from equations (15) and (18)

$$\left(1 - \frac{1}{2}\left(\frac{\alpha x}{c}\right)^2\right)\frac{\partial p_p}{\partial x} = \rho\frac{\partial}{\partial x}\left(\frac{\partial\phi}{\partial t} + \alpha x\frac{\partial\phi}{\partial x}\right) - \frac{\partial}{\partial x}\left(\rho_p\frac{\alpha^2x^2}{2}\right).$$

As $|\alpha x/c|$ is small and $\rho \simeq$ constant, the equation can be integrated to

$$p_p = \frac{\rho}{1 + \frac{1}{2}(\alpha x/c)^2}\left(\frac{\partial\phi}{\partial t} + \alpha x\frac{\partial\phi}{\partial x}\right). \tag{38}$$

The complete solution to the wave equation gives

$$\frac{\partial\phi}{\partial x} = e^{\sigma t}\left(C_A\frac{dF_A}{dx} + C_B\frac{dF_B}{dx}\right). \tag{39}$$

At the resonator plane

$$(u_p)_{x=0} = -(\partial\phi/\partial x)_0 = 0,$$

from which

$$C_A = \frac{C}{(dF_A/dx)_0}, \quad C_B = \frac{-C}{(dF_B/dx)_0},$$

$$\phi = e^{\sigma t}C\left\{\frac{F_A}{(dF_A/dx)_0} - \frac{F_B}{(dF_B/dx)_0}\right\}, \tag{40}$$

and

$$\frac{\partial\phi}{\partial x} = e^{\sigma t}C\left(\frac{dF_A/dx}{(dF_A/dx)_0} - \frac{dF_B/dx}{(dF_B/dx)_0}\right), \quad \frac{\partial\phi}{\partial t} = \sigma e^{\sigma t}C\left(\frac{F_A}{(dF_A/dx)_0} - \frac{F_B}{(dF_B/dx)_0}\right). \tag{41), (42}$$

From equations (36) and (37) it is found that

$$\left(\frac{dF_A}{dx}\right)^* = \frac{c}{\alpha}\frac{dF_A}{dx} = \frac{\mu^2}{2(1-\mu)}\left[1 + \sum_{n=2}^{\infty} A'_{n-1}\frac{(\mu-n)^2+2\mu-n}{(n-1)\,(n-\mu)}\chi\right], \tag{43}$$

where A'_{n-1} denotes the $(n-1)$th term and $A'_1 = 1$, and

$$\left(\frac{dF_B}{dx}\right)^* = \frac{c}{\alpha}\frac{dF_B}{dx} = \frac{\mu}{2}\chi^{\mu-1}\left[1 + \sum_{n=1}^{\infty} B'_{n-1}\frac{n^2-n+\mu}{n(n-1+\mu)}\chi\right], \tag{44}$$

where B'_{n-1} denotes the $(n-1)$th term and $B'_0 = 1$.

In forming the wave equation (28) it was required that $|\alpha x| \gg |\partial\phi/\partial x|$. From this an estimate of the constant C can be obtained.

From equation (40) the disturbance caused by a downstream moving perturbation—the A-component—and by the corresponding upstream moving perturbation developed by reflexion at the resonator—the B-component—can be found at any point inside the subsonic region between shock and resonator.

If a perturbation moves from the resonator upstream to the normal shock it will cause the shock to move. However, normally the pressure and velocity perturbation behind the unstable shock cannot be satisfied by the upstream moving perturbation alone and therefore a downstream moving perturbation is produced (reflected) by the shock. As the boundary conditions at the shock are different from those at the resonator, equation (40) is not valid there, but the total disturbance from the upstream moving perturbation (B-component) and the downstream moving perturbation produced by the shock (A-component) is given by

$$\phi = e^{\sigma t} C \left(k \frac{F_A}{(dF_A/dx)_0} - \frac{F_B}{(dF_B/dx)_0} \right), \tag{45}$$

from which

$$\frac{\partial \phi}{\partial x} = e^{\sigma t} C \left(k \frac{dF_A/dx}{(dF_A/dx)_0} - \frac{dF_B/dx}{(dF_B/dx)_0} \right), \tag{46}$$

$$\frac{\partial \phi}{\partial t} = \sigma e^{\sigma t} C \left(k \frac{F_A}{(dF_A/dx)_0} - \frac{F_B}{(dF_B/dx)_0} \right), \tag{47}$$

where k is a factor expressing the ratio between the amplitude of the downstream moving wave and the incident upstream moving wave.

The amplification factor k must be determined from the boundary conditions at the shock. The velocity and pressure perturbations immediately behind the shock can be found from the real parts of u_p and p_p (equations (17a) and (38)) as well as from u_{2n} and p_{2n} in the shock equations (9) and (6). As the real part of u_p contains a cosine as well as a sine term the oscillation of the shock must be the sum of a sine and a cosine oscillation, and equations (9) and (6) must be rewritten to take account of this:

$$\Delta x = l_a \sin \omega t + l_b \cos \omega t, \tag{48}$$

from which u_{2n} and p_{2n} are found.

Just behind the shock we have

$$c = a_2, \quad \alpha x/c = M_2, \quad \rho = \rho_2.$$

These are introduced into equations (36), (37), (38), (43) and (44). According to equation (32), σ is complex. The real component σ_r is a damping term. whereas the imaginary component σ_i gives the frequency of oscillation, which must be equal to ω. Here the damping is neglected and thus $\sigma_r = 0$ and $\mu = i\xi = -i\omega/\alpha$.

The coefficients to cosine and sine in the equations

$$\mathrm{Re}\, u_p = u_{2n} \quad \text{and} \quad \mathrm{Re}\, p_p = p_{2n} \tag{49), (50}$$

give four equations for the determination of possible resonance frequencies ξ, the factor of amplification k, l_a and l_b.

From the equations for the normal shock and for adiabatic flow it is found that

$$\frac{p_1}{\rho_2} \frac{2\gamma}{\gamma+1} M_1 = \frac{4a_0^2}{(\gamma+1)^2 M_1}.$$

Further the quantities

$$L_a = \omega l_a / C \quad \text{and} \quad L_b = \omega l_b / C$$

are introduced.

Then equation (49) gives for the coefficients of the cosine

$$L_a = -\operatorname{Re}\left[k\frac{(dF_A/dx)^*}{(dF_A/dx)_0^*} - \frac{(dF_B/dx)^*}{(dF_B/dx)_0^*}\right], \tag{51}$$

and for the coefficients of the sine

$$L_b = i\operatorname{Im}\left[k\frac{(dF_A/dx)^*}{(dF_A/dx)_0^*} - \frac{(dF_B/dx)^*}{(dF_B/dx)_0^*}\right], \tag{52}$$

and equation (50) gives for the coefficients of the cosine

$$\frac{4}{(\gamma+1)^2 M_1}\frac{a_0}{a_2}\left(\frac{M_1^2-2}{1+\frac{1}{2}(\gamma-1)M_1^2}\frac{dM_1}{dx}\frac{a_0}{\alpha\xi}L_b - 2\frac{a_0}{a_1}L_a\right)$$
$$= \frac{1}{1+\frac{1}{2}M_2^2}\left(-i\xi\operatorname{Im}\left[k\frac{F_A}{(dF_A/dx)_0^*} - \frac{F_B}{(dF_B/dx)_0^*}\right] - M_2 L_a\right), \tag{53}$$

and for the coefficients of the sine

$$\frac{4}{(\gamma+1)^2 M_1}\frac{a_0}{a_2}\left(\frac{M_1^2-2}{1+\frac{1}{2}(\gamma-1)M_1^2}\frac{dM_1}{dx}\frac{a_0}{\alpha\xi}L_a + 2\frac{a_0}{a_1}L_b\right)$$
$$= \frac{1}{1+\frac{1}{2}M_2^2}\left(\xi\operatorname{Re}\left[k\frac{F_A}{(dF_A/dx)_0^*} - \frac{F_B}{(dF_B/dx)_0^*}\right] + M_2 L_b\right). \tag{54}$$

These are the final equations for determination of resonance frequencies. If at a certain position of resonator and shock L_a and L_b are computed (as functions of ξ) and inserted into equations (53) and (54) each of these equations will give k as a function of ξ, and where the functions are equal to the same value, a solution to the system of equations is found.

A perturbation, which moves downstream from the shock to the resonator and is reflected there returns to the shock after a time

$$\tau = \tau_{\text{down}} + \tau_{\text{up}} = \int_{M_2(c/\alpha)}^{0}\frac{dx}{\alpha x - c} + \int_0^{M_2(c/\alpha)}\frac{dx}{\alpha x + c} = \frac{1}{-\alpha}\ln\frac{1-M_2}{1+M_2}. \tag{55}$$

After reflexion at the shock the amplitude of the perturbation, which has the frequency of resonance ω, will be multiplied by the factor k. If $|k| < 1$ the amplitude will decrease at each reflexion unless an impressed perturbation of frequency ω and of sufficiently large amplitude and suitable phase is also present.

As the shock position changes during the oscillation the value of τ also oscillates, but for small amplitudes of shock oscillation this can be disregarded.

Experimentally large-amplitude as well as small-amplitude shock oscillations have been found. Calculations carried out from the theory (see §3.5) show that $-1 \lesssim k < 1$. Thus an impressed perturbation must exist, but how it arises is not explained. A possible mechanism of generation will now be outlined.

The resonance oscillations in the central part of the jet can be expected to make the shock oscillate about a mean position as shown in figure 12(*a*).

When the resonator shock is stable its position is found to be determined essentially by the sonic line between the edge of the shock and the sonic shoulder of the resonator (figure 2). A small axial change in the position of the resonator

does not affect the form of the shock significantly, but causes a small change in its axial position. In the instability theory the perturbation introduced by equation (17*a*) was only x-oriented, i.e. a radial component of the disturbance superposed on the basic flow was not considered, but such a component must exist, which is proved by the radiation of acoustic energy from the resonant system. When such radial waves reach the above-mentioned sonic line its position is changed, and thus the position of the shock is changed. If the waves are sinusoidal it can be expected that the shock produces sinusoidal oscillations around a mean position as shown in figure 12(*b*), superposed upon the resonance

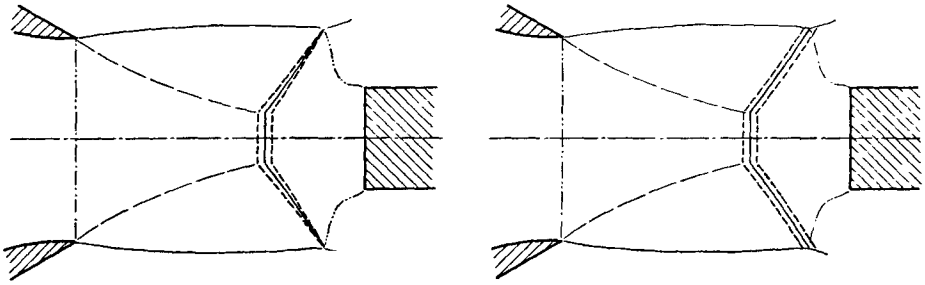

FIGURE 12. (*a*) Shock oscillation expected from resonance perturbations in the central region of the jet downstream of the shock. (*b*) Shock oscillation expected from perturbations passing the sonic line between the shock edge and sonic point of the resonator.

oscillations shown in figure 12(*a*). The shock oscillations caused by sonic line oscillations shown in figure 12(*b*) will result in impressed downstream moving perturbations originating at the shock.

When a perturbation P_a of circular frequency ω corresponding to the A-component of equation (45) leaves the shock, a short time Δt will elapse before the radial component reaches the above-mentioned sonic line and thus the impressed perturbation P_i, which is also of circular frequency ω, is delayed compared with its origin. In fact the impressed perturbation has the same nature as the normal A-component perturbation and their simultaneous values will be added. It is assumed that P_i is approximately proportional to P_A and accordingly

$$(P_i)_{t=t_1} = g(P_A + P_i)_{t=t_1-\Delta t} = g(P_A)_{t_1-\Delta t} + g^2(P_A)_{t_1-2\Delta t} + \ldots, \tag{56}$$

where g is a positive constant. If $(P_A)_{t=t_1} = \sin \omega t_1$, the total downstream moving perturbation will be

$$P_{A,\,\text{total},\,t=t_1} = (P_A + P_i)_{t=t_1} = \sin \omega t_1 + g \sin \omega(t_1 - \Delta t) + g^2 \sin \omega(t_1 - 2\Delta t) + \ldots.$$

After the time τ, $P_{A,\,\text{total},\,t=t_1}$ will appear again as a downstream moving perturbation but multiplied by the factor k:

$$(P_A)_{t=t_1+\tau} = k P_{A,\,\text{total},\,t=t_1}.$$

Here the damping by radiation of sound is disregarded. Amplification will occur if

$$|(P_A)_{t=t_1+\tau}/(P_A)_{t=t_1}| = |K| > 1,$$

i.e. if $$|k(\sin \omega t_1 + g \sin \omega(t_1 - \Delta t) + g^2 \sin \omega(t_1 - 2\Delta t) + \ldots)| > |\sin \omega t_1|.$$

If $k < 0$ it is necessary that

$$\tau \simeq (\pi/\omega)(1+2m) \quad (m = 0, 1, 2, \ldots), \tag{57a}$$

and if $k > 0$,

$$\tau \simeq (2\pi/\omega)(1+m) \quad (m = 0, 1, 2, \ldots). \tag{57b}$$

Normally it is not possible to obtain the sign of equality in equations (57a, b) and then, for example, pressure measurements at the resonator plane will show oscillations not of frequency $\omega/2\pi$ but of frequency $(2\tau)^{-1}$ for $k < 0$ and τ^{-1} for

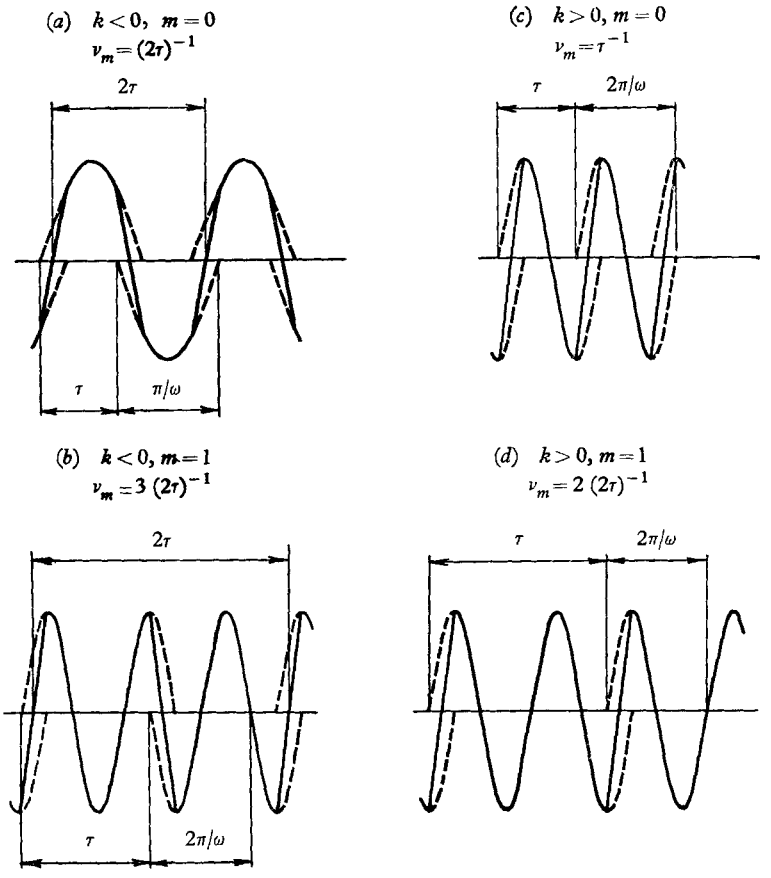

FIGURE 13. Examples of pressure oscillations caused by a casual resonance perturbation $\sin \omega t$ (duration $\simeq \tau$). For convenience the curves are made for $|K| = 1$ and it is assumed that K is proportional to k.

$k > 0$ (figure 13). However, practically it may be very difficult to determine anything but a dominating mean frequency ν_m, figure 7(a), given by

$$\nu_m = (2\tau)^{-1}(1+2m) \quad \text{for} \quad k < 0, \quad \text{and} \quad \nu_m = \tau^{-1}(1+m) \quad \text{for} \quad k > 0.$$

If several resonance frequencies are possible according to equations (53) and (54), the one for which the total amplification is the strongest will dominate the perturbations. A rather small change in the position of the resonator may influence ω, k, g and Δt sufficiently to cause a complete change of the dominating resonance frequency.

3.5. *Example of calculation*

The theory for resonance in the Hartmann generator has been applied to the case of the Hartmann generator with 7·0 mm plane resonator for which the shock-resonator positions are given in figure 4. This figure, together with figure 9, supplies sufficient information to determine at any position of the resonator the

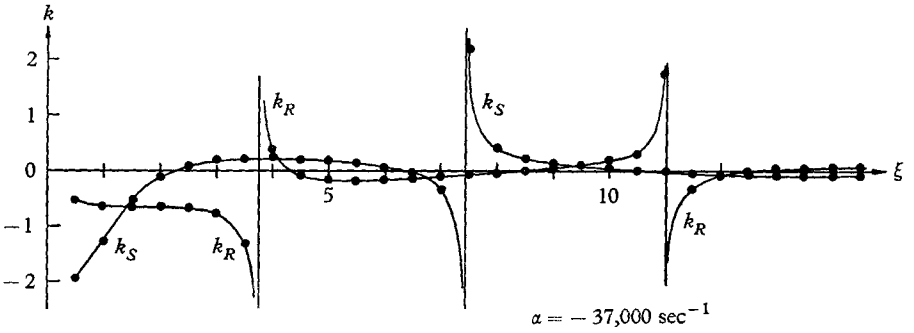

FIGURE 14. Values of k_R and k_S computed for 7·0 mm plane resonator at x_{res} = 14·8 mm (x_{sh} = 10·0 mm).

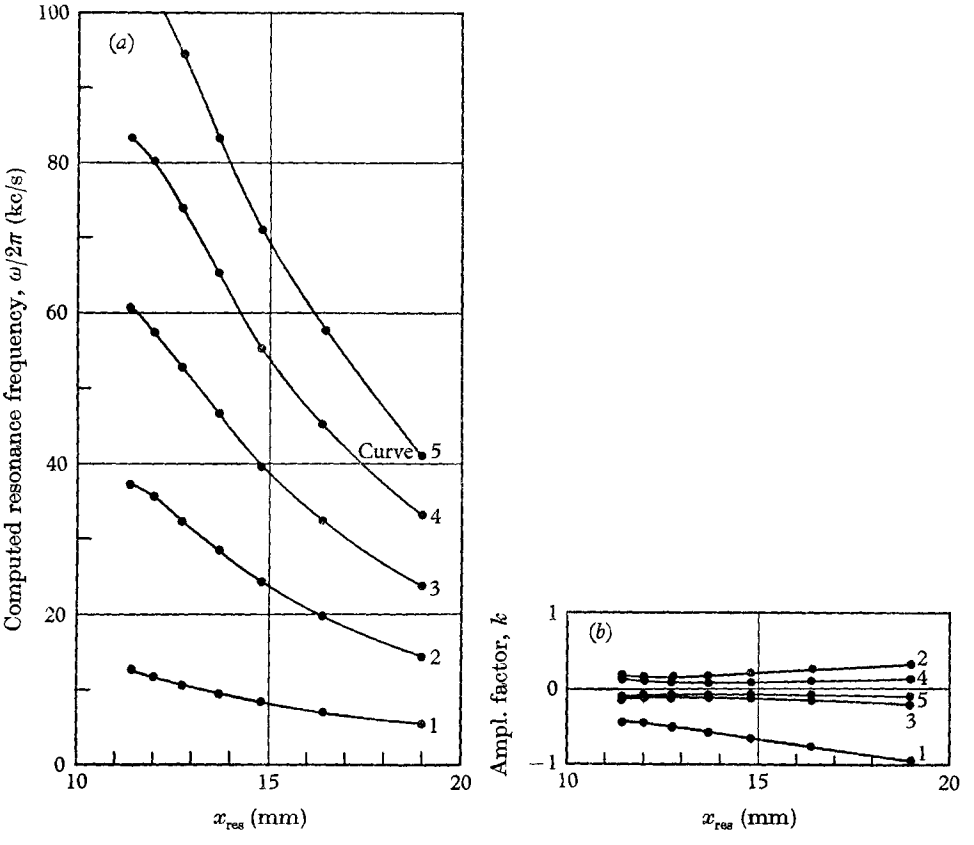

FIGURE 15. (*a*) Resonance frequencies $\omega/2\pi$ for 7·0 mm plane resonator computed from equations (53) and (54). (*b*) Corresponding values of the amplification factor k.

values of M_1, dM_1/dx, M_2, a_0/a_1, a_0/a_2 and α. As the generator is supplied with atmospheric air $\gamma = 1{\cdot}4$. The stagnation sound velocity is $a_0 = 345\,\mathrm{m/sec}$.

The values of the amplification factor k found from equations (53) and (54) are denoted k_R and k_S respectively. In figure 14, k_R and k_S are computed for the case $x_{\mathrm{res}} = 14{\cdot}8\,\mathrm{mm}$, $x_{\mathrm{sh}} = 10{\cdot}0\,\mathrm{mm}$ in the interval $\frac{1}{2} < \xi < 15$. The points of intersection give the resonance frequencies for the shock. In figure 15(*a*) these frequencies are given as functions of the resonator position and in figure 15(*b*) the corresponding values of k are found.

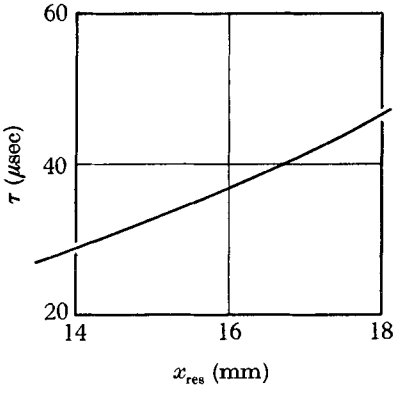

FIGURE 16. The reflexion time τ computed from equation (55) for 7·0 mm plane resonator.

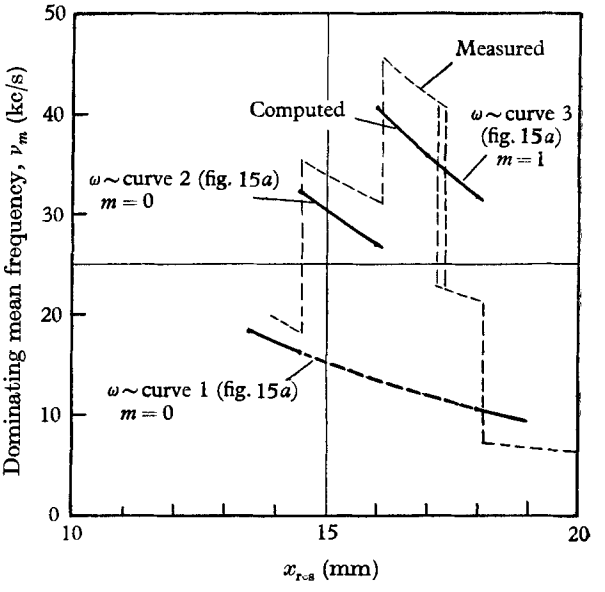

FIGURE 17. Dominating mean frequencies ν_m computed for 7·0 mm plane resonator. Computed: — — —; measured: – – – –.

It is seen that $|k|$ attains the largest value for the lowest resonance frequencies. The values of Δt and g from equation (56) cannot be determined from the general outline of the theory of impressed perturbation presented, and therefore a final determination of the dominating resonance frequency ω is not yet possible.

It is found experimentally that the dominating mean frequency ν_m at certain positions of the resonator jumps from one value to another (figure 7(*a*)) which can be explained as shifts from one resonance frequency $\omega/2\pi$ to another (figure 15(*a*)).

Computation of τ from equation (55) gives the curve shown in figure 16. As mentioned above (figure 13), τ will always be a multiple of half the period of the mean frequency, and a jump of this frequency will occur with factors as $\frac{3}{2}$, 2, $\frac{5}{2}$, 3, ... This conclusion is supported by the jumps in figure 7(*a*) except at $x_{\mathrm{res}} = 17{\cdot}3\,\mathrm{mm}$—the only resonator position at which two dominating frequencies are unmistakably superposed.

If the measured positions for frequency jumps (figure 7(*a*)) are used together with figures 15(*a*) and 16 an attempt can be made to compute the dominating

mean frequencies ν_m. This has been done in figure 17. The measured jump-factors were kept except at $x_{\text{res}} = 17{\cdot}3\,\text{mm}$, and it is then found that this point is a special one because the frequencies for $16{\cdot}1 < x_{\text{res}} < 17{\cdot}3\,\text{mm}$ and for $17{\cdot}3 < x_{\text{res}} < 18{\cdot}1\,\text{mm}$ are caused by the same resonance curve (figure 15(*a*), curve 3, $m = 1$), and no jump should be expected at all. Further for

$$x_{\text{res}} < 17{\cdot}3\,\text{mm},$$

the measured frequencies are higher than the computed ones and for

$$x_{\text{res}} > 17{\cdot}3\,\text{mm},$$

they are smaller than the computed ones. The computed value of τ (equation (55)) cannot be expected to be exact—especially for the largest amplitudes of oscillation, but it is possible that at $x_{\text{res}} = 17{\cdot}3\,\text{mm}$ the sign of the deviation just changes and this may explain the measured jump.

The author wishes to express his gratitude to Prof. K. Refslund, Prof. R. E. H. Rasmussen and Mr H. Saustrup Kristensen for valuable discussions and support.

REFERENCES

HARTMANN, J. 1939 *The Acoustic Air-Jet Generator.* Copenhagen: Ingeniørvidenskabelige Skrifter, No. 4.

KAMKE, E. 1942 *Differentialgleichungen; Lösungsmethoden und Lösungen*, pp. 465–7. Leipzig: Akademische Verlagsgesellschaft.

LIEPMANN, H. W. & ROSHKO, A. 1957 *Elements of Gasdynamics*, pp. 53, 57–9, 284–95. New York: John Wiley and Sons.

SCHLICHTING, H. 1960 *Boundary Layer Theory*, pp. 81–8. New York: McGraw-Hill.

STEWART, G. W. & LINDSAY, R. B. 1930 *Acoustics*, pp. 20–6. New York: D. van Nostrand.

VAGLIO-LAURIN, R. 1962 On the PLK method and the supersonic blunt-body problem. *J. Aerospace Sci.* **2**, 185.